Constraint on $0\nu\beta\beta$ Matrix Elements from a Novel Decay Channel of the Scissors Mode: The Case of ^{154}Gd

J. Beller,[1,*] N. Pietralla,[1] J. Barea,[2] M. Elvers,[3,†] J. Endres,[3,‡] C. Fransen,[3] J. Kotila,[4] O. Möller,[1] A. Richter,[1]
T. R. Rodríguez,[1] C. Romig,[1] D. Savran,[5,6] M. Scheck,[1,7] L. Schnorrenberger,[1] K. Sonnabend,[8]
V. Werner,[9] A. Zilges,[3] and M. Zweidinger[1]

[1]*Institut für Kernphysik, TU Darmstadt, Schlossgartenstraße 9, D-64289 Darmstadt, Germany*
[2]*Departamento de Física, Universidad de Concepción, Casilla 160-C, Concepción, Chile*
[3]*Institut für Kernphysik, Universität zu Köln, Zülpicher Straße 77, D-50937 Köln, Germany*
[4]*Center for Theoretical Physics, Sloane Physics Laboratory, Yale University, New Haven, Connecticut 06520-8120, USA*
[5]*ExtreMe Matter Institute EMMI and Research Division, GSI Helmholtzzentrum für Schwerionenforschung, Planckstraße 1,
D-64291 Darmstadt, Germany*
[6]*Frankfurt Institute for Advanced Studies FIAS, Ruth-Moufang-Straße 1, D-60438 Frankfurt am Main, Germany*
[7]*School of Engineering, University of the West of Scotland, Paisley PA1 2BE, United Kingdom*
[8]*Institut für Angewandte Physik, Goethe-Universität Frankfurt, Max-von-Laue-Straße 1, D-60438 Frankfurt, Germany*
[9]*Wright Nuclear Structure Laboratory, Yale University, New Haven, Connecticut 06520-8120, USA*
(Received 18 July 2013; revised manuscript received 29 August 2013; published 23 October 2013)

The nucleus ^{154}Gd is located in a region of the nuclear chart where rapid changes of nuclear deformation occur as a function of particle number. It was investigated using a combination of γ-ray scattering experiments and a $\gamma\gamma$-coincidence study following electron capture decay of ^{154}Tb^m. A novel decay channel from the scissors mode to the first excited 0^+ state was observed. Its transition strength was determined to $B(M1; 1^+_{sc} \rightarrow 0^+_2) = 0.031(4)\mu_N^2$. The properties of the scissors mode of ^{154}Gd imply a much larger matrix element than previously thought for the neutrinoless double-β decay to the 0^+_2 state in such a shape-transitional region. Theory indicates an even larger effect for ^{150}Nd.

The existence of massive neutrinos has been established [1–3] from neutrino-oscillation experiments. Information on their particle character, either Dirac or Majorana, and their mass could be drawn [4] from a possible observation of neutrinoless double-beta ($0\nu\beta\beta$) decays, where simultaneously a pair of protons (neutrons) converts into a pair of neutrons (protons), and from the measurement of the corresponding transition rates,

$$\lambda_{0\nu\beta\beta} = G_{0\nu}|M^{(0\nu)}|^2\left(\frac{\langle m_\nu\rangle}{m_e}\right)^2. \quad (1)$$

Here, $\langle m_\nu\rangle = \sum_k |U_{\nu k}|^2 m_k$ is the average neutrino mass and $G_{0\nu}$ is a kinematical factor. Several experiments to detect $0\nu\beta\beta$ decays are currently performed [5–10]. Nevertheless, for a determination of the neutrino mass, the nuclear matrix element (NME) $M^{(0\nu)}$ needs to be calculated sufficiently precisely from nuclear structure theory.

Calculations of $M^{(0\nu)}$ have recently been attempted using the frameworks of the nuclear shell model [11], the quasiparticle random phase approximation [12], energy density functional methods [13] (EDF), or the interacting boson model [14,15]. The latter treats pairs of protons and neutrons in terms of distinct bosons (IBM-2). The last two methods—EDF and IBM-2—are suited to describe properly the structure of open shell nuclei, where the quadrupole deformation plays a key role. The region of Nd, Sm, and Gd isotopes near $N \approx 90$ is known to be a transitional one from

spherical to prolate deformed shapes. Among these isotopes, ^{150}Nd and ^{154}Sm are possible $0\nu\beta\beta$ emitters and a reliable calculation of their NMEs requires the proper treatment of the quadrupole degree of freedom. In general, different nuclear shapes in the initial and final states lead to a reduction of the NMEs [13]. In some cases, the shape difference between the initial and final ground states enables the decay through the first excited 0^+ state of the granddaughter nucleus instead. Figure 1 shows such a decay scheme for the $\beta\beta$ decay of ^{154}Sm. Indeed, ^{150}Nd and ^{100}Mo are the only nuclei for which $2\nu\beta\beta$ decay to the first excited 0^+ state has been observed [16,17].

The $0\nu\beta\beta$ NMEs computed with EDF methods are determined by the properties of the universal effective
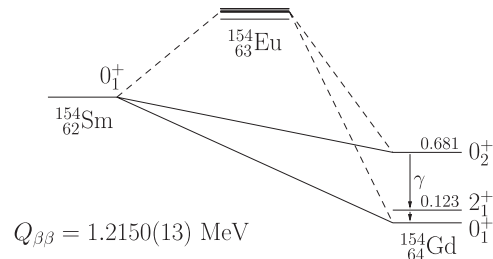

FIG. 1.   Simplified decay scheme for the $\beta\beta$ decay of ^{154}Sm. The $0\nu\beta\beta$ decay to the 0^+_2 state of ^{154}Gd could offer a coincidence tag with the prompt $0^+_2 \rightarrow 2^+_1$ and $2^+_1 \rightarrow 0^+_1$ γ rays. Excitation energies of states of ^{154}Gd are given in MeV.

interaction used in the calculation without additional adjustments. Therefore, the NMEs predicted are "parameter free" in this sense. On the other hand, the phenomenological parameters of the IBM-2 Hamiltonian must be fitted to sufficiently sensitive data. For a reliable description of $\beta\beta$ reactions, it is particularly important to verify the proper relative contributions of proton and neutron bosons to the IBM-2 wave functions. Apart from the low-energy proton-neutron symmetric states with maximum F spin, the IBM-2 predicts the existence of an entire class [18] of excited nuclear states with wave functions containing pairs of proton and neutron bosons that are coupled antisymmetrically with respect to their isospin labels. These mixed-symmetry states (MSSs) [18,19] are particularly sensitive to the proton-neutron coupling terms in the IBM-2 Hamiltonian. They exclusively restrict the three parameters of the Majorana interaction in the IBM-2 Hamiltonian. MSSs typically decay electromagnetically by comparatively strong $M1$ transitions [20,21]. Prominent examples of MSSs are the $J^\pi = 1^+$ scissors mode [22] in deformed nuclei or the mixed-symmetry $2^+_{1,ms}$ one-phonon vibration [20] in near-spherical nuclei. The spectroscopic properties of MSSs, including their excitation energies and electromagnetic decay behavior, are mandatory for a sensitive test of IBM-2 Hamiltonians used for the description of $M^{(0\nu)}$. However, information on electromagnetic transitions between MSSs and intrinsic nuclear excitations, in particular excited 0^+ states, is available only for vibrational nuclei [23].

It is the purpose of this Letter to report on the first observation of an $M1$ decay transition from the scissors mode of a predominantly axially deformed nucleus to its first excited 0^+ state, to determine the absolute $1^+_{sc} \to 0^+_2$ $M1$ strength, to improve the predictive power of the IBM-2 for the description of $M^{(0\nu)}$, to compare the results with the ones provided by EDF calculations, and to draw attention to the expected comparatively large $0\nu\beta\beta$-decay branch to excited 0^+ states in the decays of ^{154}Sm and ^{150}Nd. Measurements have been done for the nucleus ^{154}Gd, which is the final nucleus of the $\beta\beta$ decay of ^{154}Sm and very similar in structure to its $N = 90$ isotone ^{150}Nd, another nucleus considered for the search for $0\nu\beta\beta$-decay reactions [10,24]. The study of the $1^+_{sc} \to 0^+_2$ transition was made possible by an experimental approach, which for the first time made use of the population of the scissors mode of a deformed nucleus in electron capture (EC). The data represent a new significant test of the modeling of the proton-neutron degree of freedom in the structure of collective nuclear states with particular relevance for the prediction of $M^{(0\nu)}$ in the $N = 90$ region of the nuclear chart, where rapid changes of nuclear deformation occur.

Photon-scattering experiments were performed exploiting the Darmstadt high intensity photon setup [25] at the superconducting Darmstadt electron linear accelerator (S-DALINAC). For bremsstrahlung production an electron beam with an energy of $E_{e^-} = 4.5$ MeV was stopped in a radiator target made of copper. The resulting bremsstrahlung photon beam was scattered off a target of 0.579 g of Gd_2O_3 powder enriched in the isotope ^{154}Gd to 64.2%. Aluminum discs of total mass 1.572 g surrounded the target for photon flux calibration. The scattered photons were detected by three large-volume high-purity germanium (HPGe) detectors, at polar angles 90° and 130° with respect to the incoming photon beam. Figure 2 shows the (γ, γ') spectrum of ^{154}Gd recorded at incident photon energies $E_\gamma \leq 4.5$ MeV. The $J^\pi = 1^+_{sc}$ scissors mode state at 2934 keV is strongly excited. Its γ decay to the 2^+_1 state of ^{154}Gd is also clearly visible at 2811 keV. The resonant photon-scattering cross sections $I_{s,f} = g\pi^2 \lambdabar^2 \Gamma_0 \Gamma_f / \Gamma$ were measured relative to the calibration lines stemming from ^{27}Al [26], where $g = (2J + 1)/(2J_0 + 1)$ is a statistical factor and $\lambdabar = \hbar c / E_\gamma$ is the reduced scattering wavelength. $\Gamma = \hbar/\tau$ and Γ_0 (Γ_f) are the total level width and the partial decay width to the ground (final) state, which are accessible if all decay intensity ratios Γ_f/Γ are determined.

Decay intensity ratios Γ_f/Γ were measured for low-spin states of ^{154}Gd in a study of γ rays following the EC decay of the $J^\pi = 0^+$ low-spin isomer, ^{154}Tb^m [27]. The Q value of this EC process amounts to 3.56(5) MeV. In contrast to the majority of nuclides for which information on the scissors mode exists, this Q value is sufficiently large for a population of the scissors mode in the daughter nucleus ^{154}Gd in EC. The ^{154}Tb^m nuclei were produced using the fusion evaporation reaction ^{154}Gd$(p, n)^{154}$Tb^m at an energy of $E_p = 12$ MeV. The proton beam was supplied by the FN Tandem Van de Graaff accelerator at the University of Cologne. $\gamma\gamma$-coincidence events were recorded off beam with 14 HPGe detectors of the HORUS spectrometer [28]. The simultaneously recorded γ-ray singles spectrum between 2.7 and 3.0 MeV is shown in Fig. 3(a). The intense counting rate and the low background in this off-beam
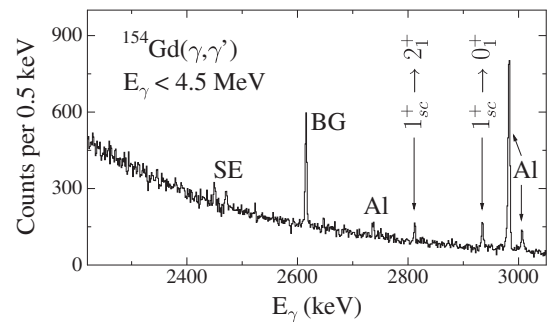

FIG. 2. Photon-scattering spectrum of ^{154}Gd. At energies of 2811 and 2934 keV, deexciting transitions from the strongly excited 1^+ state to the ground state and first 2^+ are visible. Photon-scattering cross sections are measured relative to well-known cross sections in ^{27}Al [26], which is irradiated simultaneously (marked "Al"). The labels "BG" and "SE" denote background lines or single-511 keV escape signals, respectively.
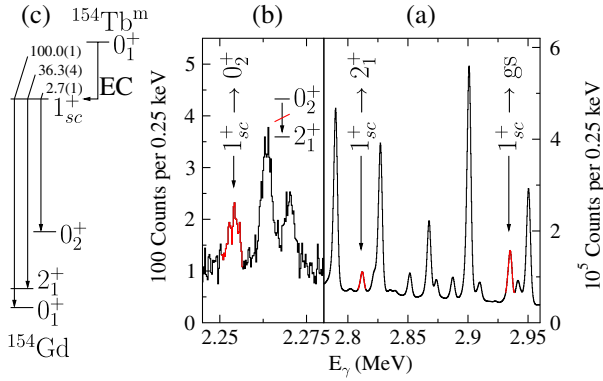
FIG. 3 (color online). (a) Part of the γ-ray spectrum recorded following the EC decay of the 0^+ low-spin isomer $^{154}\mathrm{Tb}^m$ populated in the $^{154}\mathrm{Gd}(p, n)$ reaction. (b) Part of the $\gamma\gamma$-coincidence spectrum gated on the $0_2^+ \to 2_1^+$ transition. The coincident observation of the 2253-keV transition establishes the population of the 0_2^+ state at 681 keV from the 1^+ state at 2934 keV. Please note the different scaling of the y axis. (c) Simplified decay scheme of the 1_{sc}^+ state populated in the EC decay and the respective relative decay intensities.

measurement allowed for a precise determination of the branching ratios Γ_f/Γ. The $2_1^+ \to 0_1^+$ transition amounts to 1.9×10^9 counts in singles and 1.44×10^6 counts in coincidence mode. Figure 3(b) shows the γ-ray transition at 2253 keV, which was observed in coincidence with the $0_2^+ \to 2_1^+$ transition. The 2253 keV transition depopulates the 1^+ state at 2934 keV directly to the 0_2^+ state at 681 keV. It represents the sought-after $1_{sc}^+ \to 0_2^+$ transition in $^{154}\mathrm{Gd}$ and the first observation of such a decay branch of the scissors mode in a deformed nucleus. In addition, transitions depopulating the 1_{sc}^+ state to the 1_1^- and 0_3^+ states were measured.

Combining the measured photon-scattering cross sections $I_{s,f} \propto \Gamma_0\Gamma_f/\Gamma$ and the decay intensity ratio Γ_0/Γ from the EC decay experiment, we determined partial decay widths Γ_f, total level width $\Gamma = \sum \Gamma_f$, the level lifetime $\tau = \hbar/\Gamma$, and partial transition rates $w_f = \Gamma_f/\hbar$ for the scissors mode of $^{154}\mathrm{Gd}$. The measured partial decay widths $\Gamma_{f,\pi\lambda}$ are proportional to the reduced transition strengths $B(\pi\lambda; J_i^\pi \to J_f^\pi)$. The latter are presented in Table I.

$0\nu\beta\beta$ half-lives have recently been calculated [15,16] in the framework of the IBM-2 for 16 $\beta\beta$ emitters, including the decays of $^{154}\mathrm{Sm} \to ^{154}\mathrm{Gd}$ and the $N = 90$ isotone $^{150}\mathrm{Nd} \to ^{150}\mathrm{Sm}$. NMEs of $M^{(0\nu)}[0_1^+] = 2.476$ and $M^{(0\nu)}[0_2^+] = 0.02$ were predicted for the $0\nu\beta\beta$ of $^{154}\mathrm{Sm}$ to the ground state and to the first excited 0_2^+ state of $^{154}\mathrm{Gd}$, respectively. In that study the IBM-2 Hamiltonian

$$\hat{H}_{\mathrm{IBM}} = \epsilon\hat{n}_d + \kappa\hat{Q}_\pi^\chi \cdot \hat{Q}_\nu^\chi$$
$$+ \frac{1}{2}\sum_{L=0,2} c_\pi^{(L)}[d_\pi^\dagger d_\pi^\dagger]^{(L)} \cdot [\tilde{d}_\pi \tilde{d}_\pi]^{(L)} + \hat{M}_{\pi\nu}, \quad (2)$$

TABLE I. Comparison of measured excitations energies and transition strength $B(\pi\lambda; 1_{sc}^+ \to J_f^\pi)$ of the decay channels of the scissors mode state to IBM-2 and EDF calculations together with $0\nu\beta\beta$ NMEs.

Observable	Experimental	IBM-2	EDF
$E(2_1^+)$ (MeV)	0.123[a]	0.123	0.132
$E(4_1^+)$ (MeV)	0.371[a]	0.381	0.423
$E(0_2^+)$ (MeV)	0.681[a]	0.708	0.736
$E(2_2^+)$ (MeV)	0.815[a]	0.928	0.841
$E(2_3^+)$ (MeV)	0.996[a]	1.086	$\cdots$
$E(0_3^+)$ (MeV)	1.182[a]	1.406	$\cdots$
$E(1_{sc}^+)$ (MeV)	2.934	2.934	$\cdots$
$B(M1; 1_{sc}^+ \to 0_1^+)(\mu_N^2)$	0.53(6)	0.486	
$B(M1; 1_{sc}^+ \to 2_1^+)(\mu_N^2)$	0.22(2)[b]	0.300	
$B(M1; 1_{sc}^+ \to 0_2^+)(\mu_N^2)$	0.031(4)	0.030	
$B(M1; 1_{sc}^+ \to 0_3^+)(\mu_N^2)$	0.062(10)	0.005	
$B(E1; 1_{sc}^+ \to 1_1^-)(10^{-3}\ e^2\ \mathrm{fm}^2)$	0.51(6)	$\cdots$	
$M^{(0\nu)}[0_1^+]$	$\cdots$	2.476	3.00
$M^{(0\nu)}[0_2^+]$	$\cdots$	0.374	0.63

[a]From Ref. [29].
[b]Assuming pure $M1$ character.

where the Majorana operator is defined as

$$\hat{M}_{\pi\nu} = \xi_2[d_\nu^\dagger s_\pi^\dagger - d_\pi^\dagger s_\nu^\dagger]^{(2)} \cdot [\tilde{d}_\nu s_\pi - \tilde{d}_\pi s_\nu]^{(2)}$$
$$- 2\sum_{i=1,3} \xi_i[d_\nu^\dagger d_\pi^\dagger]^{(i)} \cdot [\tilde{d}_\nu \tilde{d}_\pi]^{(i)} \quad (3)$$

was used [15,30]. Here, $\hat{n}_d$ denotes the number of d bosons, $\hat{Q}_\pi^\chi$ ($\hat{Q}_\nu^\chi$) the proton (neutron) quadrupole operator, $s_\rho^\dagger$ (s_ρ) and $d_\rho^\dagger$ ($\tilde{d}_\rho$) the s- and d-boson creation (annihilation) operators [31] and "$\cdot$" denotes the scalar product. In this framework it is possible to investigate the evolution of nuclear structure including the scissors mode and the 0_2^+ state in a region of the nuclear chart with varying quadrupole deformation such as near $N = 90$ isotones. The parameters used in [14,15] were adjusted [32] in such a way that key characteristics of the experimental level schemes and transition probabilities for Gd nuclei known at the time were reproduced. However, no experimental information on the 1^+ scissors mode was known at the time when the IBM-2 parameters were fitted to data [32]. The new data on the 1^+ scissors mode and its decay behavior allow us to fix the parameters ξ_i of the Majorana operator. While the Majorana operator has little influence on the energy eigenvalues of the low-lying full-symmetric states, it significantly affects the wave function of the 0_2^+ state of the previous calculation and also the $M^{(0\nu)}[0_2^+]$ NME. An accurate description of the 1_{sc}^+ excitation energy within the IBM-2 has a dramatic impact on $M^{(0\nu)}[0_2^+]$. A similar analysis as in [33] leads to the parameter set $\epsilon = 0.596$, $\kappa = -0.078$, $c_\pi^{(0)} = -0.20$, $c_\pi^{(2)} = -0.10$, $\xi_2 = 0.2325$, $\xi_1 = \xi_3 = 0.3875$ MeV, and $\chi = -1.0$. The Majorana parameters were set to satisfactorily reproduce the

excitation energy of the 1_{sc}^+ state and its $M1$-decay branching to the 0_2^+ state.

For the calculation of absolute $B(M1)$ transition strengths, effective g factors were kept to the free orbital values $g_\nu = 0$ for neutron bosons and $g_\pi = 1\mu_N$ for proton bosons, respectively. A comparison of experimental and theoretical level energies and $M1$ transition strengths can be found in Table I. Theory agrees now with the data on the observed electromagnetic decays of the scissors mode to the lowest-lying levels within a factor of two. Figure 4 shows a comparison between IBM-2 and experiment and for $M1$ and $0\nu\beta\beta$ matrix elements, where available.

Taking the new experimental information on the scissors mode of ^{154}Gd into account, the IBM-2 calculation for the $0\nu\beta\beta$ NMEs yields $M^{(0\nu)}[0_2^+] = 0.374$, more than one order of magnitude larger than previously calculated. The NME for ground state to ground state $0\nu\beta\beta$ decay of ^{154}Sm to ^{154}Gd is not affected and robustly remains at $M^{(0\nu)}[0_1^+] = 2.5$. The significantly larger NME for the $0\nu\beta\beta$ decay to an excited 0_2^+ state implies that one may consider measuring the $0\nu\beta\beta$ decay in coincidence with the γ decay of the 0_2^+ state (see Fig. 1). This option may help to reduce the background by coincidence conditions and increase the sensitivity towards detection of $0\nu\beta\beta$ decay events.

Next, we compare our results with those from EDF methods. In this framework [13,34], the NMEs can be expressed as

$$M^{(0\nu)} = \iint g_i^*(\beta_i)\tilde{m}(\beta_i, \beta_f)g_f(\beta_f)d\beta_i d\beta_f \quad (4)$$

$$= \int \bar{m}^{(0\nu)}(\beta)d\beta, \quad (5)$$

where $\beta_{i(f)}$ and $g_{i(f)}(\beta_{i(f)})$ are the quadrupole deformation and the collective wave function, which accounts for the contribution of a given deformation in the initial (final) state, respectively. $\tilde{m}(\beta_i, \beta_f)$ is the NME as a function of

the initial and final deformation and $\bar{m}^{(0\nu)}(\beta) \equiv \int \tilde{m}(\beta_i, \beta)g_i^*(\beta_i)d\beta_i$. In deformed nuclei, $\tilde{m}(\beta_i, \beta_f) \approx \delta(\beta_i - \beta_f)$ [13] and the NMEs are determined basically by the overlaps between the initial and final wave functions. If the ground states are similar in mother and granddaughter nuclei, such a NME is maximum—as it happens in mirror nuclei [34]—being almost zero to excited 0^+ states by orthonormalization. However, this is different in the present case as it is shown in Fig. 5(a). The deformed ground state of ^{154}Sm is narrower, and it peaks at a slightly larger deformation than for ^{154}Gd. Hence, the overlap and the NME between ^{154}Sm ground state and the β-vibrational first excited 0^+ state of ^{154}Gd have finite values. The accumulated integrals

$$\bar{M}^{(0\nu)}(\beta) = \int_{-\infty}^{\beta} \bar{m}^{(0\nu)}(\beta')d\beta' \quad (6)$$

plotted in Fig. 5(b) show that while the NME for the ground state is strictly increasing from $\beta = 0.2$ to 0.4, where it reaches almost its final value, the NME for the excited state is suppressed due to its change in sign but not fully canceled out. The final values for the NME are $M^{(0\nu)}[0_1^+] = 3.03$ and $M^{(0\nu)}[0_2^+] = 0.62$, rather close to the improved IBM-2 ones.

Subsequent emissions of $0_2^+ \rightarrow 2_1^+$ and $2_1^+ \rightarrow 0_1^+$ γ rays in coincidence with the population of the first excited 0^+ state in $0\nu\beta\beta$ reactions could offer a coincidence tag for the $0\nu\beta\beta$-decay channel to the 0_2^+ final state. In the case of the ^{154}Sm $\rightarrow$ ^{154}Gd $0\nu\beta\beta$ decay, the NME, despite an increase by an order of magnitude, may still be too small for the decay to be observable in practice. The calculated ratio of
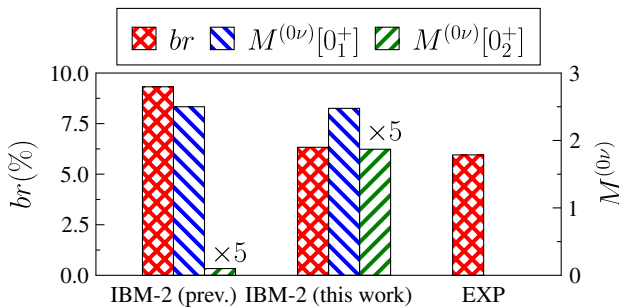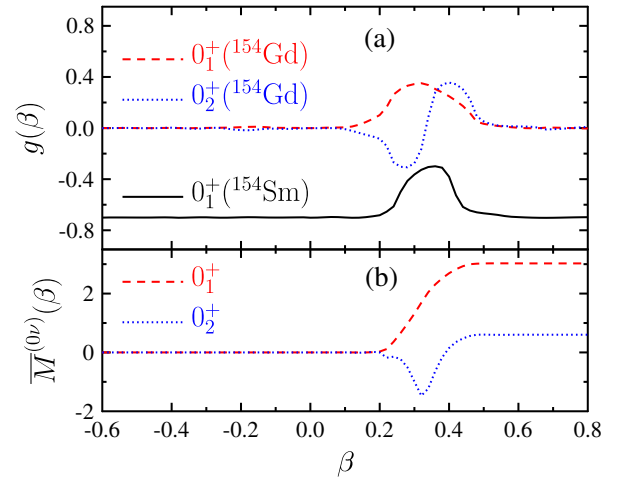
FIG. 4 (color online). Comparison of the $B(M1)$ branching ratio $br = B(M1; 1_{sc}^+ \rightarrow 0_2^+)/B(M1; 1_{sc}^+ \rightarrow 0_1^+)$ in % (red) of the 1^+ scissors mode state of ^{154}Gd, the dimensionless $0\nu\beta\beta$ NME $M^{(0\nu)}[0_1^+]$ (blue), and $M^{(0\nu)}[0_2^+]$ (green) for previous [15] and new IBM-2 parameters and experimental data, where available.

FIG. 5 (color online). (a) Collective wave functions for the initial ^{154}Sm ground state (black solid) and the final 0_1^+ (red dashed) and 0_2^+ (blue dotted) states of ^{154}Gd as a function of the quadrupole deformation (β). (b) Accumulated NMEs for transitions from ^{154}Sm to the ground (red dashed) and first excited 0^+ (blue dotted) states of ^{154}Gd.

partial transition rates [Eq. (1)] $\lambda_{0\nu\beta\beta}[0_2^+]/\lambda_{0\nu\beta\beta}[0_1^+] = G_{0\nu}(0_2^+)|M^{(0\nu)}[0_2^+]|^2/(G_{0\nu}(0_1^+)|M^{(0\nu)}[0_1^+]|^2)$ are 0.0021 for the IBM-2 and 0.0041 for the EDF calculation. However, this situation changes in the ^{150}Nd $\rightarrow$ ^{150}Sm $0\nu\beta\beta$ decay. There, the ratio of the phase-space factors [35] $G_{0\nu}(0_1^+)/G_{0\nu}(0_2^+)$ is considerably larger (0.43 instead of 0.09) and the more pronounced change in deformation between mother and granddaughter nucleus increases the $M^{(0\nu)}[0_2^+]$ NME. Indeed, EDF calculations for this decay amount to $M^{(0\nu)}[0_1^+] = 1.71$ and $M^{(0\nu)}[0_2^+] = 2.81$. The ratio of the partial transition rates is $\lambda_{0\nu\beta\beta}[0_2^+]/\lambda_{0\nu\beta\beta}[0_1^+] = 1.2$, implying an about equally strong $0\nu\beta\beta$ decay to the excited state, which enables an additional coincidence tag for background suppression.

In summary, we have measured the $M1$ transition strengths between the scissors mode and an intrinsic excitation in a deformed rotational nucleus for the first time. We have obtained the $B(M1; 1_{sc}^+ \rightarrow 0_2^+)$ value in ^{154}Gd from a combination of photon-scattering experiments for the identification of the 1_{sc}^+ state and the measurement of its Γ_0^2/Γ value and from $\gamma\gamma$-coincidence experiments, following EC for the measurement of decay branching ratios Γ_f/Γ. The new data are particular sensitive to the proton-neutron interaction of the IBM-2, and it allowed for an improvement of the previous parameter set needed for an accurate description of ^{154}Gd within the IBM-2 framework. The latter results in an increase of the prediction for the $0\nu\beta\beta$-decay NME of ^{154}Sm to the 0_2^+ state of ^{154}Gd by an order of magnitude. An even stronger relative $0\nu\beta\beta$-decay branch to the 0_2^+ state must be expected for the decay of its $N = 90$ isotone ^{150}Nd.

*beller@ikp.tu-darmstadt.de
†Present address: Sirona Dental Systems GmbH, D-64625 Bensheim, Germany.
‡Present address: Areva NP GmbH, D-63067 Offenbach-Kaiserlei, Germany.

[1] Y. Fukuda *et al.* (Super-Kamiokande Collaboration), Phys. Rev. Lett. **81**, 1562 (1998).
[2] Q. R. Ahmed *et al.* (SNO Collaboration), Phys. Rev. Lett. **89**, 011302 (2002).
[3] K. Eguchi *et al.* (KamLAND Collaboration), Phys. Rev. Lett. **90**, 021802 (2003).
[4] F. T. Avignone, S. R. Elliott, and J. Engel, Rev. Mod. Phys. **80**, 481 (2008).
[5] C. Arnaboldi *et al.* (CUORICINO Collaboration), Phys. Rev. C **78**, 035502 (2008).
[6] N Ishihara *et al.*, J. Phys. Conf. Ser. **203**, 012071 (2010).
[7] M. Auger *et al.* (EXO Collaboration), Phys. Rev. Lett. **109**, 032505 (2012).
[8] GERDA Collaboration *et al.*, J. Phys. G **40**, 035110 (2013).
[9] A. Gando *et al.* (KamLAND-Zen Collaboration), Phys. Rev. C **85**, 045504 (2012).
[10] R. Arnold *et al.*, Eur. Phys. J. C **70**, 927 (2010).
[11] J. Menéndez, A. Poves, E. Caurier, and F. Nowacki, Nucl. Phys. **A818**, 139 (2009).
[12] F. Šimkovic, A. Faessler, H. Müther, and V. Rodin, M. Stauf, Phys. Rev. C **79**, 055501 (2009).
[13] T. R. Rodríguez and G. Martínez-Pinedo, Phys. Rev. Lett. **105**, 252503 (2010).
[14] J. Barea and F. Iachello, Phys. Rev. C **79**, 044301 (2009).
[15] J. Barea, J. Kotila, and F. Iachello, Phys. Rev. C **87**, 014315 (2013).
[16] A. S. Barabash, P. Hubert, A. Nachab, and V. I. Umatov, Phys. Rev. C **79**, 045501 (2009).
[17] M. J. Hornish, L. De Braeckeleer, A. S. Barabash, and V. I. Umatov, Phys. Rev. C **74**, 044314 (2006).
[18] F. Iachello, Phys. Rev. Lett. **53**, 1427 (1984).
[19] P. Van Isacker, K. Heyde, J. Jolie, and A. Sevrin, Ann. Phys. (N.Y.) **171**, 253 (1986).
[20] N. Pietralla, P. von Brentano, and A. F. Lisetskiy, Prog. Part. Nucl. Phys. **60**, 225 (2008).
[21] K. Heyde, P. von Neumann-Cosel, and A. Richter, Rev. Mod. Phys. **82**, 2365 (2010).
[22] D. Bohle, A. Richter, W. Steffen, A. E. L. Dieperink, N. Lo Iudice, F. Palumbo, and O. Scholten, Phys. Lett. B **137**, 27 (1984).
[23] G. Rusev *et al.*, Phys. Rev. Lett. **95**, 062501 (2005).
[24] J. Argyriades *et al.* (NEMO Collaboration), Phys. Rev. C **80**, 032501(R) (2009).
[25] K. Sonnabend *et al.*, Nucl. Instrum. Methods Phys. Res., Sect. A **640**, 6 (2011).
[26] N. Pietralla *et al.*, Phys. Rev. C **51**, 1021 (1995).
[27] D. C. Sousa, L. L. Riedinger, E. G. Funk, and J. W. Mihelich, Nucl. Phys. **A238**, 365 (1975).
[28] A. Linnemann, Ph.D. thesis, University of Cologne, 2005.
[29] C. W. Reich, Nucl. Data Sheets **110**, 2257 (2009).
[30] J. Barea, J. Kotila, and F. Iachello, Phys. Rev. Lett. **109**, 042501 (2012).
[31] F. Iachello and A. Arima, *The Interacting Boson Model* (Cambridge University Press, Cambridge, England, 1987).
[32] O. Scholten, Ph.D. thesis, University of Groningen, 1980.
[33] J. Kotila, K. Nomura, L. Guo, N. Shimizu, and T. Otsuka, Phys. Rev. C **85**, 054309 (2012).
[34] T. R. Rodríguez and G. Martínez-Pinedo, Phys. Lett. B **719**, 174 (2013).
[35] J. Kotila and F. Iachello, Phys. Rev. C **85**, 034316 (2012).